

Article

Kinetics Study on the Modification Process of Al₂O₃ Inclusions in High-Carbon Hard Wire Steel by Magnesium Treatment

Xingqiang Xiong^{1,2}, Changrong Li^{1,2,*}, Zuobing Xi^{1,2} and Lu Chen^{1,2}

¹ School of Materials and Metallurgy, Guizhou University, Guiyang 550025, China; xxq15223673790@163.com (X.X.); bingzxi@163.com (Z.X.); chen841283779@163.com (L.C.)

² Guizhou Key Laboratory of Metallurgical Engineering and Process Energy Conservation, Guiyang 550025, China

* Correspondence: crli@gzu.edu.cn

Abstract: The aim of the experiment in this work is to modify the Al₂O₃ inclusions in high-carbon hard wire steel by magnesium treatment. The general evolution process of inclusions in steel is: Al₂O₃ → MgO·Al₂O₃(MA) → MgO. The unreacted core model was used to study the modification process of inclusions. The results show that the complete modification time (t_f) of inclusions is significantly shortened by the increase of magnesium content in molten steel. For Al₂O₃ inclusions with radius of 1 μm and Mg content in the range of 0.0005–0.0055%, the modification time of Al₂O₃ inclusions to MA decreased from 755 s to 25 s, which was reduced by 730 s. For Al₂O₃ inclusions with a radius of 1.5 μm and Mg content in the range of 0.001–0.0035%, the Al₂O₃ inclusions were completely modified to MgO inclusions from 592 s to 55 s. The Mg content in the molten steel increased 3.4-fold, and the time for complete modification of inclusions was shortened by about 10-fold. With the increase of Al and O content in molten steel, the complete modification time increased slightly, but the change was small. At the same time, the larger the radius of the unmodified inclusion is, the longer the complete modification time is. The t_f of Al₂O₃ inclusions with a radius of 1 μm when modified to MA is 191 s, and the t_f of Al₂O₃ inclusions with a radius of 2 μm when modified to MA is 765 s. According to the boundary conditions and the parameters of the unreacted core model, the MgO content in inclusions with different radius is calculated. The experimental results are essentially consistent with the kinetic calculation results.

Keywords: high-carbon hard wire steel; inclusions; magnesium treatment; unreacted core model



Citation: Xiong, X.; Li, C.; Xi, Z.; Chen, L. Kinetics Study on the Modification Process of Al₂O₃ Inclusions in High-Carbon Hard Wire Steel by Magnesium Treatment. *Metals* **2021**, *11*, 1560. <https://doi.org/10.3390/met11101560>

Academic Editor: Minkyu Paek

Received: 23 August 2021

Accepted: 24 September 2021

Published: 29 September 2021

Publisher's Note: MDPI stays neutral with regard to jurisdictional claims in published maps and institutional affiliations.



Copyright: © 2021 by the authors. Licensee MDPI, Basel, Switzerland. This article is an open access article distributed under the terms and conditions of the Creative Commons Attribution (CC BY) license (<https://creativecommons.org/licenses/by/4.0/>).

1. Introduction

Hard wire, also known as hard wire rod, is usually known as high-carbon hard wire for high-quality carbon structural steel with a carbon content of not less than 0.6%. The alumina nonmetallic inclusions in hard wire steel have an important influence on the fatigue resistance of wire breaking or hard wire products during cold drawing, resulting in early fracture of steel in practical application [1–3]. The number, size, type and distribution of alumina inclusions are very important for the properties of hard wire steels [4–8]. The solubility of magnesium in molten steel is relatively high. Magnesium has a strong affinity with oxygen and sulfur, which can effectively reduce the content of O and S in steel, and improve the quantity and morphology of inclusions in steel; moreover, it has an obvious modification effect on oxide inclusions and plays a role in purifying molten steel [9–14].

A great deal of research has been conducted on the kinetics and thermodynamics of calcium and magnesium treatment [13,15–18]. Yang et al. [19] added magnesium to 35CrNi3MoV steel to treat inclusions and found that magnesium treatment can effectively reduce the number of inclusions, and the MgO inclusions are spherical. The spherical MgO inclusions are small in size, dispersed in the molten steel, not easy to aggregate, and have little effect on the properties of the steel. Ma et al. [20] studied Al₂O₃ inclusions in magnesium-treated bearing steel. The irregularly shaped Al₂O₃ inclusions in molten

steel were modified into MgAl_2O_4 or spherical MgO inclusions. However, excessive magnesium content is not conducive to controlling the total oxygen content in the molten steel, and further control of the magnesium content is required. Yu et al. [21] studied the composition and changes of inclusions in magnesium-treated medium-manganese steels with different aluminum contents. When the aluminum content in the steel is greater than 0.0076%, $\text{MnO}\cdot\text{Al}_2\text{O}_3$ inclusions are transformed into Al_2O_3 inclusions. With the increase of aluminum content in molten steel, the molar ratio of $\text{MgO}/\text{Al}_2\text{O}_3$ in inclusions decreases. When the aluminum content in the molten steel is less than 0.2%, unstable MgO inclusions are formed in the molten steel. Takata et al. [22] conducted experiments by passing Mg steam into aluminum deoxidized steel and found that the oxygen content in molten steel decreased rapidly. One reason for this is the strong deoxidization reaction of Mg , however in contrast, the bubbles generated promote the floating and discharging of inclusions. Through the SEM-EDS analysis of inclusions in as-cast steel at different times, it is found that Mg has effectively modified the alumina inclusions. The inclusions in as-cast steel are mainly MgO and magnesia-alumina spinels ($\text{MgO}\cdot\text{Al}_2\text{O}_3$) inclusions, and the size of inclusions decreases with time.

In this paper, based on the dynamic model of Al_2O_3 inclusion modification by calcium treatment studied by the research group [23], the multi-layer unreacted core model of Al_2O_3 inclusion in magnesium-treated steel was carried out, and the step-by-step reaction dynamic model of Al_2O_3 inclusion modification in high-carbon hard wire steel under the condition of magnesium treatment was established. The relationship between the change of solute element content, inclusion conversion rate, inclusion radius, and MgO content in inclusion and inclusion modification time was discussed in detail, which can better reveal the process and mechanism of Al_2O_3 inclusion modification in magnesium treatment.

2. Experimental Method

2.1. Experiment Procedure

The composition design of the raw materials in this experiment is based on the chemical element composition in SWRH62A steel, and the batching smelting is carried out on this basis. The experiment was carried out in a tubular resistance furnace. The corundum crucible containing industrial pure iron, ferrosilicon alloy and electrolytic manganese was placed in the constant temperature zone and heated to $1600\text{ }^\circ\text{C}$ by electric heating. After molten steel was melted, aluminum alloy was added for deoxidation. After 300 s, Mg-Ni alloy was added. Subsequently, a quartz tube was used to draw three samples after adding magnesium (60 s, 300 s, 600 s). The sample taken out is put into the sodium chloride solution for cooling, and argon gas is introduced into the furnace during the smelting process, and the flow rate is maintained at 5 min/L. The order of alloy addition and sampling in the current experiment is shown in Figure 1. The amount of Mg-Ni alloy added in the two experiments is different. Table 1 lists the composition of the raw materials used in this study.

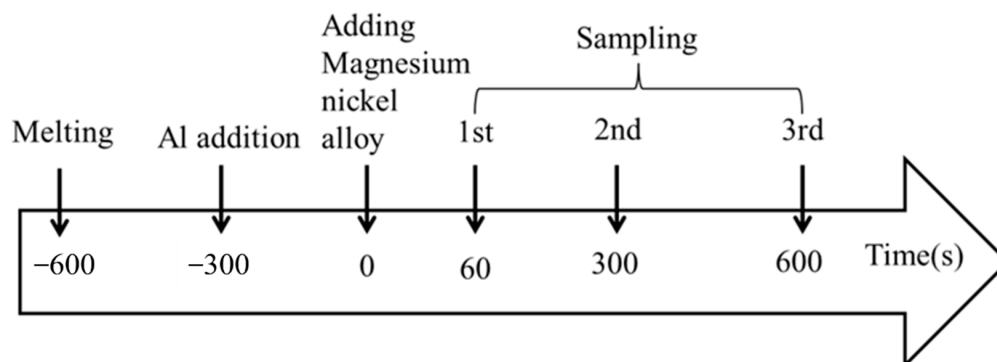


Figure 1. The alloy addition and sampling plan in the experiment.

Table 1. Raw material composition (mass/%).

Raw Material	Fe	Si	Mn	S	C	Mg	Ni	Al	Others
Industrial pure iron	99.7	0.02	0.03	0.0002	0.0018	-	-	0.001	0.2445
electrolytic manganese	-	-	99.999	-	-	-	-	-	0.001
Si-Fe alloy	21	78	0.4	0.02	0.1	-	-	-	0.48
Al alloy	0.7	0.8	0.15	-	-	-	-	96.94	1.41
Mg-Ni alloy	0.01	0.01	20.44	0.01	-	21.41	58.12	-	-
QT400	95.8	0.17	0.5	0.01	3.45	-	-	-	0.07

2.2. Detection and Analysis Method

Inductively coupled plasma emission spectrometer (ICP-MS) was used to determine the content of Mg and Al in the experimental steel, the content of C, Si, Mn and S in the experimental steel was measured by a direct-reading spectrometer, and the content of O was measured by an inorganic oxygen and hydrogen tester. After the experiment, the sample was ground on the grinder and polished on the polishing machine. A German Zeiss SIGMA+X-Max20 (Baden-Wuerttemberg, Germany) scanning electron microscope (SEM) and energy dispersive spectrometer (EDS) were used to analyze the two-dimensional morphology and internal composition of inclusions in the sample section.

3. Experimental Results and Analysis

3.1. Chemical Composition of Steel

Table 2 lists the measured composition of each element in the two furnaces of experimental steel. Due to the different addition amounts of Mg-Ni alloy, there is a significant difference in the mass fraction of Mg in the two experiments. The analysis results show that the Mg content in M1 steel is 0.001%, while the Mg content in M2 steel is 0.0018%.

Table 2. Chemical composition of different experimental steels (mass/%).

Number	C	Si	Mn	S	O	Al	Mg
M1	0.652	0.183	0.312	0.0021	0.0057	0.0048	0.001
M2	0.652	0.183	0.300	0.0017	0.0045	0.0051	0.0018

3.2. Composition and Morphology of Inclusions

After aluminum deoxidation, high-carbon hard wire steel is added with Mg-Ni alloy for Mg treatment. Figure 2 shows the composition distribution diagram of the inclusions in the sample. Through the analysis of the EDS dot composition, it can be determined that the inclusions are mainly Al_2O_3 (whiter in color), and $\text{MgO}\cdot\text{Al}_2\text{O}_3$ (black in color) around the inclusions. The morphology of the inclusions is more consistent with the unreacted core model. From (a) to (c) in Figure 2, it can be seen that the area of the black area gradually increases, and the area of the white area gradually decreases, indicating that with the diffusion of Mg element in the molten steel, Al_2O_3 inclusions are completely transformed into $\text{MgO}\cdot\text{Al}_2\text{O}_3$.

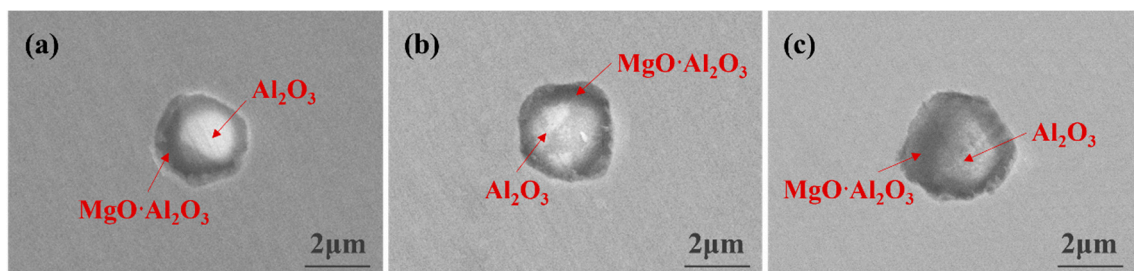
**Figure 2.** The composition distribution diagram of the inclusions in the sample. (a) sample M1, (b) sample M2, (c) sample M2.

Figure 3 is a morphology diagram of typical inclusions in sample M1, and Figure 4 is a morphology diagram of typical inclusions in sample M2. After Mg treatment, the cross-sectional morphology of the inclusions in the steel tends to be round, which has a modification effect on the irregular morphology of the inclusions.

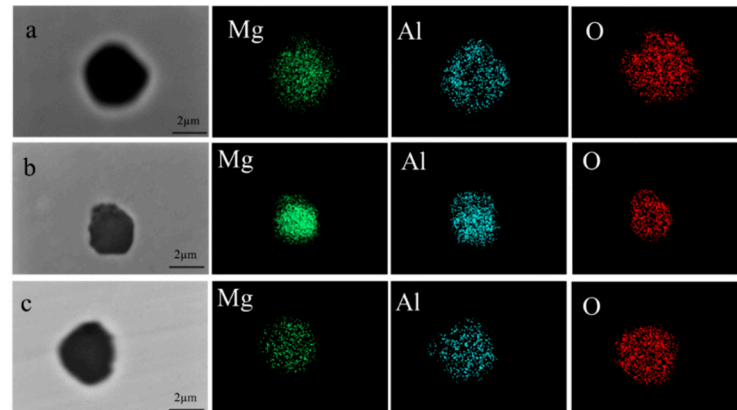


Figure 3. Morphology of typical inclusions in sample M1 ((a): 60 s; (b): 300 s; (c): 600 s).

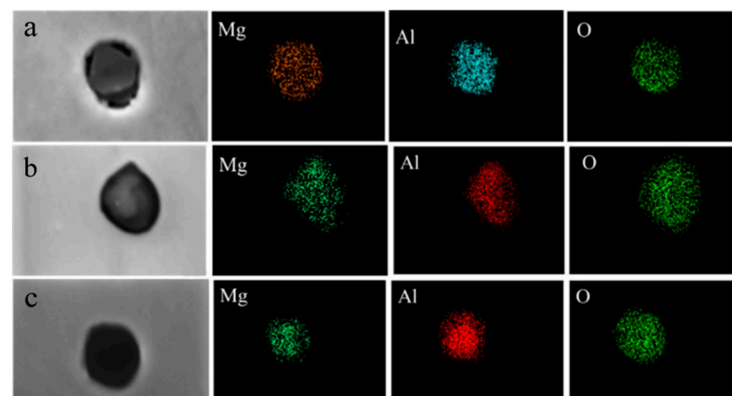


Figure 4. Morphology of typical inclusions in sample M2 ((a): 60 s; (b): 300 s; (c): 600 s).

25 inclusions were detected in each sample for composition statistics. Figure 5 shows the proportion of MgO in steel detected 60 s, 300 s, and 600 s after Mg was added to M1 and M2. In the M1 sample, when the Mg-Ni alloy is added for 60 s, the mass fraction of MgO in the calcium aluminate inclusions is in the range of 18.39–32.71%, and the average content of MgO in the inclusions is 25.47%. When added for 300 s, the mass fraction of MgO in the inclusions is 24.89–46%, and the average content of MgO in the inclusions increased to 32.38%. When added for 600 s, the mass fraction of MgO in the inclusions is in the range of 31.94–54.94%, and the average content of MgO in the inclusions increases to 43.47%. In the M2 sample, when the Mg-Ni alloy is added for 60 s, the mass fraction of MgO in the calcium aluminate inclusions is in the range of 22.84–47.72%, and the average content of MgO in the inclusions is 38.68%. When added for 300 s, the mass fraction of MgO in the inclusions is in the range of 40.52–61.73%, and the average content of MgO in the inclusions increases to 49.95%. When added for 600 s, the mass fraction of MgO in the inclusions is in the range of 51.39–72.97%, and the average content of MgO in the inclusions increases to 63.6%.

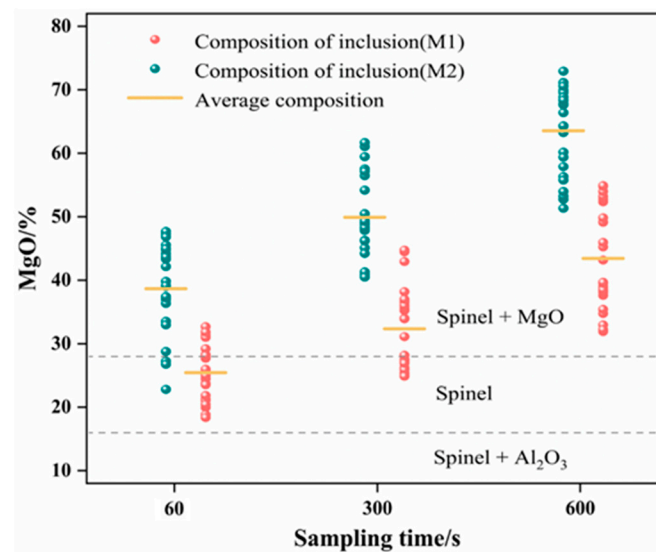


Figure 5. Inclusion composition detected after adding magnesium in high-carbon hard wire steel.

4. Dynamic Model Establishment

In order to describe the mass transfer of the Al_2O_3 inclusion modification process in the magnesium-treated high-carbon hard wire steel, based on the unreacted core model, the morphology and composition of the inclusions in Figures 2–4 were explored. In order to facilitate the calculation, it is assumed that all the inclusions are spherical in shape.

- (1) Before magnesium treatment, the shape of Al_2O_3 inclusion in the high-carbon hard wire molten steel is spherical.
- (2) The temperature of molten steel is very high, assuming that the interface reaction can quickly balance.
- (3) In order to simplify the discussion of the model, it is assumed that the concentrations of magnesium, aluminum, and oxygen in the molten steel are constant.
- (4) It is assumed that the diffusion of all substances in the magnesium aluminate layer is steady-state diffusion, which conforms to Fick's first law, and the actual diffusion mechanism in molten steel is more complicated.

As shown in Figure 6, during the magnesium treatment process, Mg in the high-carbon hard wire molten steel first diffuses to the surface of Al_2O_3 inclusions, forming an $\text{MgO}\cdot\text{Al}_2\text{O}_3$ layer on the surface of the Al_2O_3 inclusions. With the diffusion of Mg elements in the molten steel, the Al_2O_3 inclusions are completely converted to $\text{MgO}\cdot\text{Al}_2\text{O}_3$. The Mg element continues to diffuse in the $\text{MgO}\cdot\text{Al}_2\text{O}_3$ inclusions, and the $\text{MgO}\cdot\text{Al}_2\text{O}_3$ inclusions form an MgO layer on the surface, and finally the $\text{MgO}\cdot\text{Al}_2\text{O}_3$ inclusions are completely transformed into MgO inclusions.

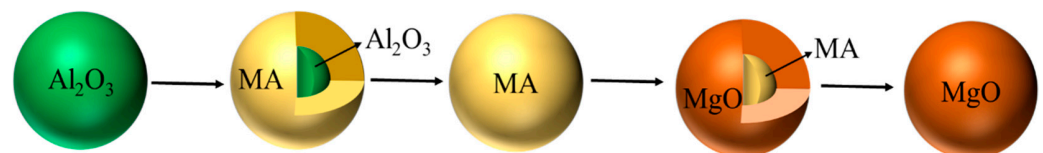


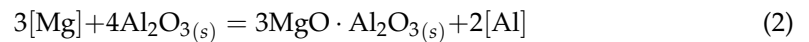
Figure 6. Reaction model of Al_2O_3 inclusion in high-carbon hard wire steel treated by magnesium.

Taking the transformation of Al_2O_3 inclusions into MA as an example, the description is divided into the following three steps (Figure 7 is a schematic diagram of the transformation).

- (1) The Mg in the high-carbon hard wire molten steel diffuses to the Al_2O_3 layer/steel interface, and the reaction formula is:



- (2) [Mg] reacts with Al_2O_3 inclusions on the surface:



- (3) [Al] generated by the reaction diffuses outward through the MA layer and enters the molten steel.

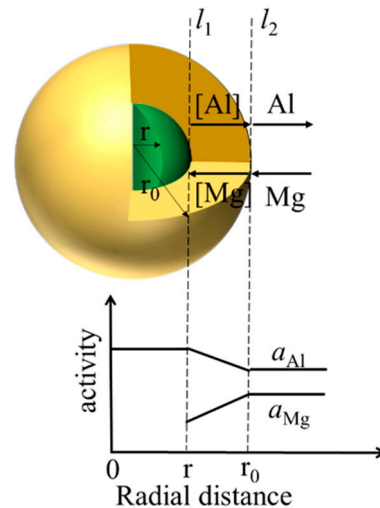


Figure 7. Schematic diagram of modification of Al_2O_3 inclusions into $\text{MgO} \cdot \text{Al}_2\text{O}_3$ inclusions.

4.1. The Diffusion of Al in the Magnesium Aluminate Layer Is the Limiting Link in the Modification Process of Inclusions

The diffusion rate of Al in the MA layer is expressed as:

$$v_{\text{Al}} = -\frac{dn_{\text{Al}}}{dt} = 4\pi r^2 D_{\text{Al}} \frac{dc_{\text{Al}}}{dr} \quad (3)$$

In Formula (3): n_{Al} represents the amount of Al material, mol; r represents the radius of unreacted core MA, μm ; D_{Al} represents the diffusion rate of Al in molten steel, m^2/s ; c_{Al} is the concentration of Al in MA, mol/m^3 ; t Represents the modification time of inclusions, s.

$$dc_{\text{Al}} = -\frac{1}{4\pi r^2 D_{\text{Al}}} \frac{dn_{\text{Al}}}{dt} \frac{dr}{r^2} \quad (4)$$

The integral of Formula (4) is:

$$\int_{c_{\text{Al},l_1}}^{c_{\text{Al},l_2}} dc_{\text{Al}} = -\frac{1}{4\pi r^2 D_{\text{Al}}} \frac{dn_{\text{Al}}}{dt} \int_r^{r_0} \frac{dr}{r^2} \quad (5)$$

From Formula (5):

$$v_{\text{Al}} = -\frac{dn_{\text{Al}}}{dt} = 4\pi D_{\text{Al}} \frac{r_0 r}{r_0 - r} (c_{\text{Al},l_1} - c_{\text{Al},l_2}) \quad (6)$$

In Formula (6): c_{Al,l_1} represents the concentration of Al at the interface of two inclusions, and c_{Al,l_2} represents the concentration of Al at the interface between the inclusions MA and molten steel. It can be seen from Formula (6) that the rate of Al consumption in the modification reaction during Mg treatment is:

$$-\frac{dn_{\text{Al}}}{dt} = -\frac{2dn_{\text{Al}_2\text{O}_3}}{dt} = -\frac{4\pi r^2 \rho_{\text{Al}_2\text{O}_3}}{M_{\text{Al}_2\text{O}_3}} \frac{dr}{dt} \quad (7)$$

In Formula (7): $\rho_{\text{Al}_2\text{O}_3}$ represents the density of Al_2O_3 , $\rho_{\text{Al}_2\text{O}_3} = 3.5 \times 10^3 \text{ kg}/\text{m}^3$, $M_{\text{Al}_2\text{O}_3}$ represents the molar mass of Al_2O_3 , $M_{\text{Al}_2\text{O}_3} = 102 \text{ g}/\text{mol}$.

Combining Formulas (6) and (7), we can get:

$$\int_0^t \frac{M_{\text{Al}_2\text{O}_3} D_{\text{Al}} (c_{\text{Al},l_1} - c_{\text{Al},l_2})}{\rho_{\text{Al}_2\text{O}_3}} dt = \int_{r_0}^r \left(r - \frac{r^2}{r_0} \right) dr \quad (8)$$

After sorting out, the relationship between the unreacted core radius of inclusions and the modification time (t) is:

$$t = \frac{\rho_{\text{Al}_2\text{O}_3} r_0^2}{6M_{\text{Al}_2\text{O}_3} D_{\text{Al}} (c_{\text{Al},l_1} - c_{\text{Al},l_2})} \left[1 - 3\left(\frac{r}{r_0}\right)^2 + 2\left(\frac{r}{r_0}\right)^3 \right] \quad (9)$$

In order to facilitate the calculation of the modification time of inclusions, the activity of each solute element in the steel is used instead of its concentration. The Formula (9) can be expressed as:

$$t = \frac{\rho_{\text{Al}_2\text{O}_3} r_0^2}{6M_{\text{Al}_2\text{O}_3} D_{\text{Al}} (a_{\text{Al},l_1} - a_{\text{Al},l_2})} \left[1 - 3\left(\frac{r}{r_0}\right)^2 + 2\left(\frac{r}{r_0}\right)^3 \right] \quad (10)$$

When Al_2O_3 inclusions are completely transformed into $\text{MgO} \cdot \text{Al}_2\text{O}_3$, that is, $r = 0$, the complete modification time (t_f) of inclusions is:

$$t_f = \frac{\rho_{\text{Al}_2\text{O}_3} r_0^2}{6M_{\text{Al}_2\text{O}_3} D_{\text{Al}} (a_{\text{Al},l_1} - a_{\text{Al},l_2})} \quad (11)$$

It is known that $\rho_{\text{Al}_2\text{O}_3}$, $M_{\text{Al}_2\text{O}_3}$, and D_{Al} are all constants, and the modification time of Al_2O_3 inclusions depends on the radius and the difference in Al activity between the two interfaces of the inclusions.

4.2. Assuming That the Diffusion of Mg in Inclusions Is the Limiting Link in the Modification Process

The diffusion rate of Mg in the MA layer is expressed as:

$$v_{\text{Mg}} = \frac{dn_{\text{Mg}}}{dt} = 4\pi r^2 D_{\text{Mg}} \frac{dc_{\text{Mg}}}{dr} \quad (12)$$

In Formula (7): n_{Mg} represents the amount of Mg, mol; r represents the radius of the unreacted core Al_2O_3 , μm ; D_{Mg} represents the diffusion rate of Mg in molten steel, m^2/s ; C_{Mg} is the concentration of Mg in MA, mol/m^3 ; t represents the modification time of inclusions, s.

$$dc_{\text{Mg}} = \frac{1}{4\pi r^2 D_{\text{Mg}}} \frac{dn_{\text{Mg}}}{dt} \frac{dr}{r^2} \quad (13)$$

The integral of Formula (13) is:

$$\int_{C_{\text{Mg},l_1}}^{C_{\text{Mg},l_2}} dc_{\text{Mg}} = \frac{1}{4\pi r^2 D_{\text{Mg}}} \frac{dn_{\text{Mg}}}{dt} \int_r^{r_0} \frac{dr}{r^2} \quad (14)$$

From Formula (14):

$$v_{\text{Mg}} = \frac{dn_{\text{Mg}}}{dt} = 4\pi D_{\text{Mg}} \frac{r_0 r}{r_0 - r} (c_{\text{Mg},l_1} - C_{\text{Mg},l_2}) \quad (15)$$

In Formula (15): c_{Mg,l_1} represents the concentration of Mg at the interface between Al_2O_3 inclusions and MA inclusions, and C_{Mg,l_2} represents the concentration of Mg at the interface between MA inclusions and molten steel.

The rate at which Mg is generated by the modification reaction is:

$$\frac{dn_{\text{Mg}}}{dt} = \frac{2dn_{\text{MgO}}}{dt} = \frac{x_{\text{MgO}} dn_{\text{MA}}}{dt} = \frac{20}{71} \frac{4\pi r^2 \rho_{\text{MA}}}{M_{\text{MA}}} \frac{dr}{dt} \quad (16)$$

In Formula (16): ρ_{MA} represents the density of $MgO \cdot Al_2O_3$, $\rho_{MA} = 3.57 \times 10^3 \text{ kg/m}^3$, M_{MA} represents the molar mass of $MgO \cdot Al_2O_3$, $M_{MA} = 142 \text{ g/mol}$.

Combining Formulas (15) and (16), we can get:

$$\int_0^t \frac{71M_{MA}D_{Mg}(c_{Mg,l_1} - c_{Mg,l_2})}{20\rho_{MA}} dt = \int_{r_0}^r (r - \frac{r^2}{r_0}) dr \quad (17)$$

After sorting out, the relationship between the unreacted core radius of inclusions and the modification time (t) is:

$$t = \frac{40\rho_{MA}r_0^2}{211M_{MA}D_{Mg}(c_{Mg,l_1} - c_{Mg,l_2})} \left[1 - 3\left(\frac{r}{r_0}\right)^2 + 2\left(\frac{r}{r_0}\right)^3 \right] \quad (18)$$

In order to facilitate the calculation of the modification time of inclusions, the activity of each element in the steel is used instead of its concentration. The Formula (18) can be expressed as:

$$t = \frac{40\rho_{MA}r_0^2}{211M_{MA}D_{Mg}(a_{Mg,l_1} - a_{Mg,l_2})} \left[1 - 3\left(\frac{r}{r_0}\right)^2 + 2\left(\frac{r}{r_0}\right)^3 \right] \quad (19)$$

When the Al_2O_3 inclusions are completely transformed into MA, that is, $r = 0$, the complete modification time (t_f) of the inclusions is:

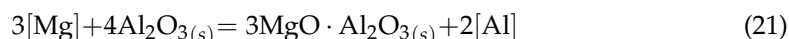
$$t_f = \frac{40\rho_{MA}r_0^2}{211M_{MA}D_{Mg}(a_{Mg,l_1} - a_{Mg,l_2})} \quad (20)$$

4.3. Determination of Kinetic Model Parameters

4.3.1. It Is Assumed That the Diffusion of Al in the Magnesium Aluminate Layer Is the Limiting Link in the Modification Process of Inclusions

The concentration of [Al] in calcium aluminate inclusions is difficult to determine, and can be replaced by activity. Because the activity data is complete, it can be assumed that the solution obeys Raoult law, using '1wt% standard state' for calculation.

Interface l_1 :



The Gibbs free energy of this reaction is:

$$\Delta G^\theta = 618,182 - 456.93T, \text{ J} \cdot \text{mol}^{-1} \quad (22)$$

$$\Delta G^\theta = -RT \ln K^\theta = -RT \ln \frac{a_{Al,l_1}^2 a_{MgO \cdot Al_2O_3}}{a_{Mg}^3 a_{Al_2O_3}^4} \quad (23)$$

$$a_{Al,l_1} = \left[\frac{a_{Mg}^3 a_{Al_2O_3}^4}{a_{MgO \cdot Al_2O_3}^3} \exp\left(\frac{\Delta G^\theta}{-RT}\right) \right]^{\frac{1}{2}} \quad (24)$$

In Formula (24): a_{Al,l_1} represents the activity of Al in the interface layer between Al_2O_3 inclusions and $MgO \cdot Al_2O_3$, and the sum of $a_{Al_2O_3}$ and $a_{MgO \cdot Al_2O_3}$ is 1.

Interface l_2 :

$$a_{Al,l_2} = f_{Al} \times [\%Al] \quad (25)$$

4.3.2. It Is Assumed That the Diffusion of Mg in the Magnesium Aluminate Layer Is the Limiting Link in the Modification Process of Inclusions

Interface l_1 :

$$a_{\text{Mg},l_1} = \left[\frac{a_{\text{Al}}^2 a_{\text{MgO} \cdot \text{Al}_2\text{O}_3}^3}{a_{\text{Al}_2\text{O}_3}^4 \exp\left(\frac{\Delta G^\theta}{-RT}\right)} \right]^{\frac{1}{3}} \quad (26)$$

In Formula (26): a_{Mg,l_1} represents the activity of the interfacial layer Mg between Al_2O_3 inclusions and $\text{MgO} \cdot \text{Al}_2\text{O}_3$.

Interface l_2 :

$$a_{\text{Mg},l_2} = f_{\text{Mg}} \times [\% \text{Mg}] \quad (27)$$

In Formula (27): a_{Mg,l_2} represents the activity of Mg at the interface between $\text{MgO} \cdot \text{Al}_2\text{O}_3$ inclusions and molten steel.

According to the interface reaction (12), combining the composition of the experimental steel in Table 2 and the interaction coefficient between elements in the molten steel at 1873K in Table 3, Formulas (24) and (27) are used to calculate a_{Mg} and a_{Al} in the experimental steel (as shown in Table 4).

Table 3. Interaction coefficient of Mg, O and Al at 1873 K (1600 °C) [24,25].

e_i^j	C	Si	Mn	S	O	Al	Mg
O	−0.42	−0.066	−0.021	−0.13	−0.17	−1.17	−1.98
Al	0.091	0.056	−0.004	0.0035	−1.98	0.0043	−0.13
Mg	−0.31	−0.088	-	-	−3	−0.12	-

Table 4. Activity of Mg and Al in sample M1 and sample M2.

Number	a_{Mg}	a_{Al}
M1	0.000581	0.005473
M2	0.001054	0.005846

4.4. Dynamic Model Results and Analysis

4.4.1. Determination of Restrictive Links

Since there are multiple dynamic steps involved in the model, a restrictive analysis is carried out to study the influence of each step on the modification time of inclusions.

According to Formulas (11) and (20), the diffusion of Al and Mg in the magnesium aluminate layer is calculated as the limiting link for the modification of alumina inclusions. The calculation results are shown in Figure 8. When the radius of the MA inclusions is 2 μm : Al diffusion in the MA layer is the limiting link, and t_f is 246 s; Mg diffusion in the MA layer is the limiting link, and t_f is 765 s. The t_f when the diffusion of Mg in the MA layer is the limiting link is greater than the t_f when the diffusion of Al in the MA layer is the limiting link, so the diffusion of Mg in the inclusion layer is considered to be the limiting link in the inclusion modification process.

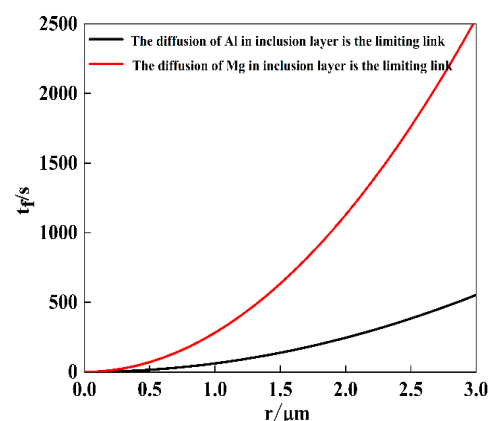


Figure 8. Diffusion of Mg and Al in magnesium aluminate layer is the limiting link of modification process.

4.4.2. The Effect of Solute Element Content in Molten Steel on Modification Time

The content of the solute element in the molten steel changes, so that the activity of the element changes, and the time for the complete modification of the inclusions changes accordingly. According to Formulas (11), (20) and (27), the content changes of Mg, Al, and O in molten steel are calculated. The complete modification time required for the transformation of Al_2O_3 inclusions with $r = 1 \mu\text{m}$ into $\text{MgO}\cdot\text{Al}_2\text{O}_3$ is shown in Figure 9. As the magnesium content in molten steel increases, the time for complete modification of inclusions is significantly shortened. When the Mg content is in the range of 0.0005–0.0055%, the de-modification time of Al_2O_3 inclusions into $\text{MgO}\cdot\text{Al}_2\text{O}_3$ is reduced from 755 s to 25 s, which is a decrease of 730 s. With the increase of Al and O content in molten steel, the complete modification time increases slightly, but the change is small. The Mg concentration in molten steel has the greatest influence on the modification time of inclusions. The high Mg environment in molten steel facilitates the transformation of Al_2O_3 inclusions into $\text{MgO}\cdot\text{Al}_2\text{O}_3$ inclusions.

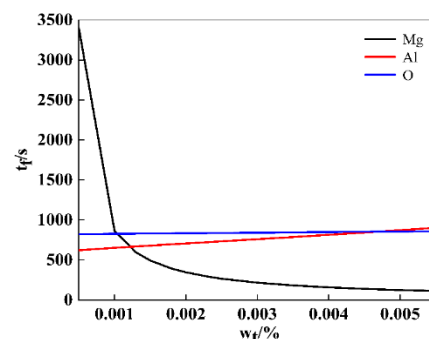


Figure 9. Effect of solute element content in high-carbon hard wire steel on the time of complete modification of Al_2O_3 inclusions to $\text{MgO}\cdot\text{Al}_2\text{O}_3$.

In fact, these concentrations cannot be changed independently; they are determined by the balance of steel and inclusions, and any change is accompanied by other kinds of changes to achieve balance. Indeed, these calculations are only to determine the importance of the transportation steps. According to Formulas (20), (26) and (27), the relationship between the Mg content in molten steel of high-carbon hard wire steel and the modification time of inclusions is calculated, as shown in Figure 8.

With the increase of magnesium content in molten steel, the time for complete modification of inclusions is significantly shortened. Take the inclusion with a radius of $r = 1.5 \mu\text{m}$ as an example: when the Mg content in the molten steel is 0.001%, it takes 430 s for the Al_2O_3 inclusions to be completely transformed into MA inclusions, as shown in Figure 10a, and 162 s for MA inclusions to be completely transformed into MgO inclusions, as shown in Figure 10b. When the magnesium content in the molten steel is 0.0035%, it takes 40 s for Al_2O_3 inclusions to be completely transformed into MA inclusions, and 15 s for MA inclusions to be completely transformed into MgO inclusions. The magnesium content in molten steel increased 3.4-fold, and the complete modification time of inclusions was shortened by approximately 10-fold. High-carbon hard wire molten steel contains low magnesium content, and the modification process of inclusions is relatively slow, with an increase of magnesium content in molten steel promoting the modification of inclusions. Therefore, the amount of magnesium added should be reasonably controlled in the actual production process.

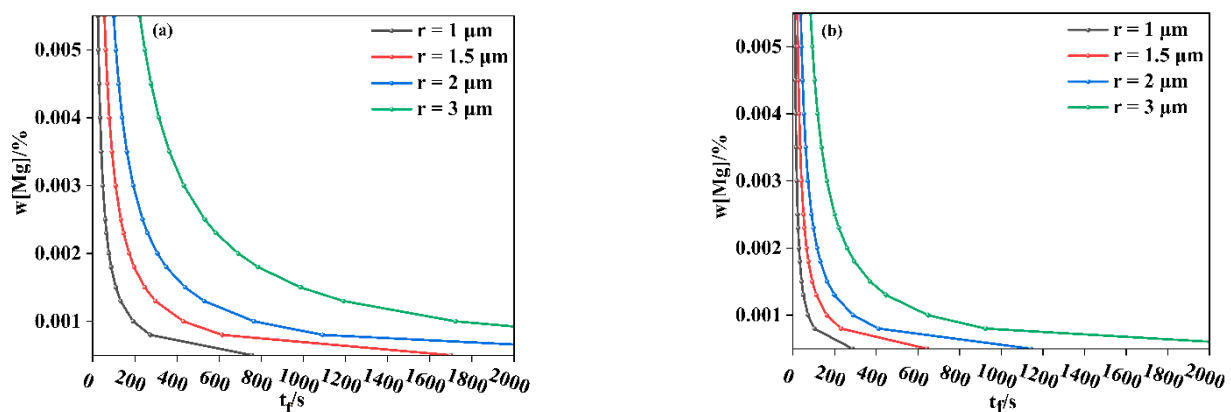


Figure 10. Relationship between Mg content in molten steel and complete modification time of inclusions with different compositions. (a) sample M1, (b) sample M2.

4.4.3. Influence of Inclusion Conversion Rate in High-Carbon Hard Wire Steel on Modification Time

After the Ni-Mg alloy is added to the molten steel, the magnesium diffuses in the molten steel to the surface of the Al_2O_3 inclusions to react with them, and the Al_2O_3 inclusions are modified. The conversion rate of inclusions is expressed as (taking the conversion of Al_2O_3 to MA as an example):

$$\alpha = \frac{m_{\text{Al}_2\text{O}_3(\text{beginning})} - m_{\text{Al}_2\text{O}_3(\text{end})}}{m_{\text{Al}_2\text{O}_3(\text{beginning})}} \times 100\% \quad (28)$$

According to Formulas (19) and (28), the relationship between the conversion rate and the modification time during the modification inclusions is calculated, as shown in Figure 11. When the inclusions are initially modified, the modification rate is faster, and as the reaction progresses, the modification rate gradually slows down. Take the inclusion with radius $r = 2 \mu\text{m}$ as an example: in Figure 11a, when 50% of Al_2O_3 inclusions are transformed into MA, the required modification time is 85 s; when the remaining 50% of Al_2O_3 inclusions are transformed into MA, the required modification time is 680 s; in Figure 11b, when 50% of the MA inclusions are converted to MgO , the required modification time is 32 s; when the remaining 50% of the MA inclusions are converted to MgO , the required modification time is 256 s. When different types of inclusions are transformed, the modification time required for the inclusion conversion rate from 50% to complete modification is about eight times that of the conversion rate from 0 to 50%. Therefore, in the late stage of inclusion modification, stirring rate should be improved to promote inclusion modification and reduce modification time.

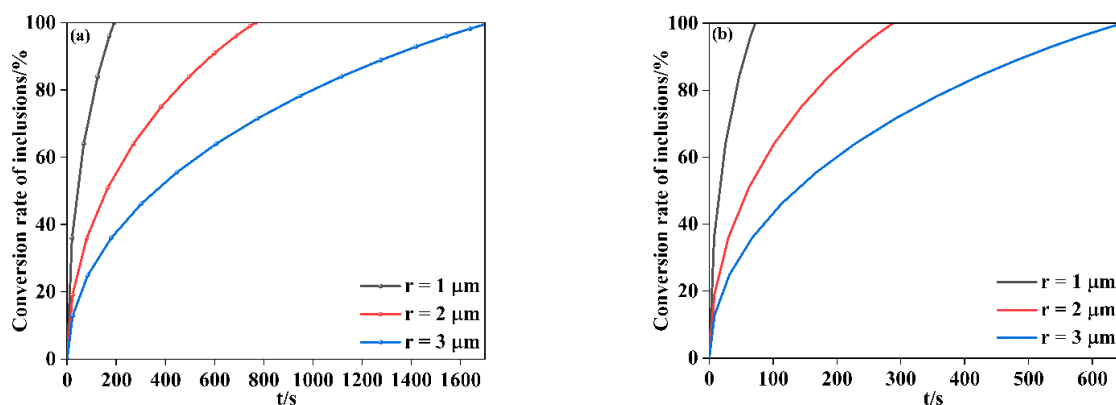


Figure 11. Modification process of inclusions with different particle sizes ((a). Al_2O_3 modified into MA; (b). MA is modified into MgO).

4.4.4. The Relationship between the Radius of Inclusions and the Time of Modification

As shown in Figure 12, the complete modification time increases as the radius of the inclusion increases. It can be seen from Formula (20) that the complete modification time of inclusions is proportional to the square of its radius. Take the complete modification of Al_2O_3 inclusions into MA inclusions as an example: Al_2O_3 inclusions with a radius of $r = 1 \mu\text{m}$ require a complete modification time of 191 s, and Al_2O_3 inclusions with a radius of $r = 2 \mu\text{m}$ require a complete modification time of 765 s. The larger the radius of the undenatured inclusions, the longer the time required for complete modification. Al_2O_3 inclusions with a radius less than $5 \mu\text{m}$ in molten steel can be transformed into $\text{MgO}\cdot\text{Al}_2\text{O}_3$ inclusions in 4783 s. When the radius of inclusions in molten steel is less than $5 \mu\text{m}$, $\text{MgO}\cdot\text{Al}_2\text{O}_3$ can all be transformed into MgO inclusions within 1800 s. When the radius of the inclusions is the same, the modification time required for the transformation of Al_2O_3 inclusions into MgO inclusions is the longest.

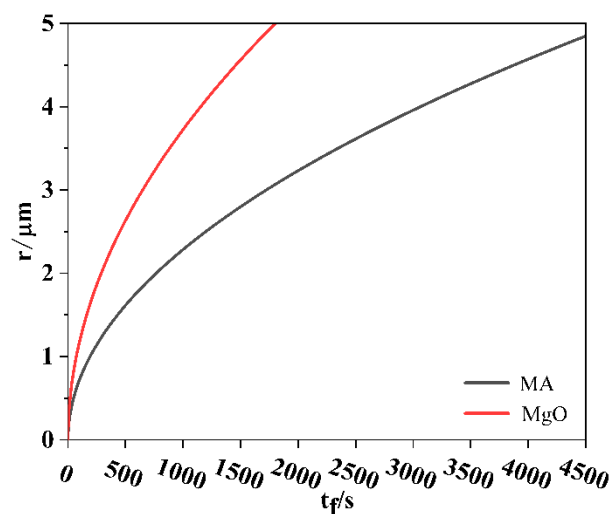


Figure 12. Complete modification time of Al_2O_3 inclusions with different sizes.

4.5. Model Validation

The average radius of the inclusions in the experimental steel is within $1\text{--}3 \mu\text{m}$. According to the boundary conditions and unreacted core model parameters, the MgO content in the inclusions of different radius is calculated over time. The results are shown in Figure 13, (a) is the theoretical value of M1, (b) is the theoretical value of M2.

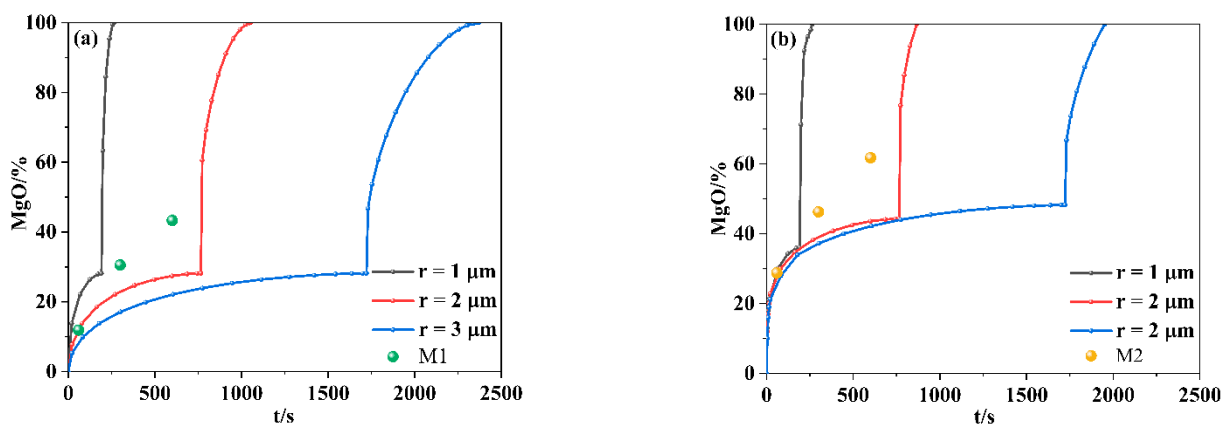


Figure 13. Variation of MgO content in inclusions with time. (a) sample M1, (b) sample M2.

Compare the theoretical value with the test value of the inclusions in Section 3.2 of the text. In M1, when the MgO content in the inclusions is higher than 28%, the modification time required for the inclusions is significantly shortened. The above kinetic

model calculates that the MgO content in the inclusions with a radius of 2 μm is 11.9%, and requires magnesium treatment for 56 s. This may be due to the existence of large-sized inclusions in the experimental steel, which cannot be modified into MgO·Al₂O₃ inclusions. After 300 s of magnesium treatment, the average content of MgO in inclusions is 30.55%, which is close to the average content of MgO 32.38% after 300 s of magnesium treatment in the experiment. After 600 s of magnesium treatment, the average content of MgO in inclusions is 30.55%, which is close to the average MgO content of 43.47% after 600 s of magnesium treatment in the experiment. After magnesium treatment for 120 s, the average radius of inclusions is basically less than 2 μm . The experimental results in M1 are basically consistent with the calculated results of the kinetic model.

In M2, when the MgO content in inclusions is higher than 42%, the required modification time of inclusions is significantly shortened. After 60 s of magnesium treatment, the average content of MgO in the inclusions was 29.25%, which was nearly 10% different from the 38.68% of the average MgO content after 300 s of magnesium treatment in the experiment, which may be affected by large-size inclusions. After 300 s of magnesium treatment, the average content of MgO in inclusions was 46.26%, which was close to the average content of 49.95% of MgO after 300 s of magnesium treatment in the experiment. After 600 s of magnesium treatment, the average content of MgO in inclusions was 61.77%, which was close to the average MgO content of 63.6% after 600 s of magnesium treatment in the experiment. After 60 s of magnesium treatment, the average radius of inclusions in the steel is essentially less than 2 μm . The experimental results in M2 are essentially consistent with the calculated results of the kinetic model. In summary, the kinetic model calculations after magnesium treatment in M1 and M2 are ultimately consistent with the experimental values.

5. Conclusions

- (1) Through the analysis of the restrictive link, the influence of each step on the modification time of inclusions is determined, and it is concluded that the t_f , when the diffusion of Mg in the MA layer is the limiting link, is greater than the t_f when the diffusion of Al in the MA layer is the limiting link. Thus, it is considered that the diffusion of Mg in the inclusion layer is the limiting link in the modification process of the inclusion.
- (2) As the magnesium content in the molten steel increases, the time for complete modification of inclusions is significantly shortened. The content of Al and O in molten steel increases, and the complete modification time increases slightly, but the change is small. The Mg concentration in molten steel has the greatest influence on the modification time of inclusions. The high Mg environment in molten steel facilitates the transformation of Al₂O₃ inclusions into MgO·Al₂O₃ inclusions.
- (3) When the inclusions are initially denatured, the modification rate is faster, and as the reaction progresses, the modification rate gradually slows down. Therefore, in the late stage of modification of inclusions, the stirring rate should be increased to promote modification of inclusions and reduce the time of modification.
- (4) The complete modification time of the inclusions increases with the increase of the radius of the inclusions. When the radius of the inclusions is the same, the modification time required for the Al₂O₃ inclusions to be transformed into MgO·Al₂O₃ inclusions is the longest.
- (5) According to the boundary conditions and the parameters of the unreacted core model, the MgO content in the inclusions of different radius was calculated over time, and the experimental results were essentially consistent with the calculation results of the kinetic model.

Author Contributions: Conceptualization, X.X., Z.X. and C.L.; methodology, X.X., Z.X. and C.L.; software, X.X.; formal analysis, X.X., Z.X. and L.C.; writing—original draft preparation, X.X., Z.X. and L.C.; writing—review and editing, X.X., Z.X. and C.L.; funding acquisition, X.X., Z.X. and

L.C.; funding acquisition, C.L. All authors have read and agreed to the published version of the manuscript.

Funding: This project is financially supported by the National Science Foundation of China with the grant No. 52074095, 51864013.

Institutional Review Board Statement: Not applicable.

Informed Consent Statement: Not applicable.

Data Availability Statement: The data used to support the findings of this study are available from the corresponding authors upon reasonable request.

Conflicts of Interest: The authors declare no conflict of interest.

References

1. Pilarczyk, J.W.; Muskalski, Z.; Dyja, P.; Golis, B. Influence of non-metallic inclusions on drawability of high carbon steel wire rod. *Wire J. Int.* **2002**, *35*, 81–85.
2. Ji, S.L.; Lee, K.H.; Yang, Y.S.; Lee, C.Y.; Bae, C.M.; Kim, B.M. The Effects of Non-Metallic Inclusion on Ductile Damage of High Carbon Steel Wire in Multi-Pass Dry Drawing Process. *Key Eng. Mater.* **2014**, *622*, 155–161. [[CrossRef](#)]
3. Tanaka, Y.; Pahlevani, F.; Kitamura, S.-Y.; Privat, K.; Sahajwalla, V. Behaviour of Sulphide and Non-alumina-Based Oxide Inclusions in Ca-Treated High-Carbon Steel. *Met. Mater. Trans. A* **2020**, *51*, 1384–1394. [[CrossRef](#)]
4. Chen, L.; Chen, W.; Hu, Y.; Chen, Z.; Xu, Y.; Yan, W. Effects of K₂CO₃ Addition on Inclusions in High-Carbon Steel for Saw Wire. *High Temp. Mater. Process.* **2018**, *37*, 701–709. [[CrossRef](#)]
5. Khurana, B.; Spooner, S.; Rao, M.B.V.; Roy, G.G.; Srirangam, P. In situ Observation of Calcium Oxide Treatment of Inclusions in Molten Steel by Confocal Microscopy. *Met. Mater. Trans. A* **2017**, *48*, 1409–1415. [[CrossRef](#)]
6. Bejjani, R.; Collin, M.; Thersleff, T.; Odelros, S. Multi-scale study of initial tool wear on textured alumina coating, and the effect of inclusions in low-alloyed steel. *Tribol. Int.* **2016**, *100*, 204–212. [[CrossRef](#)]
7. Dub, A.V.; Volkov, V.G.; Romashkin, A.N.; Gordeev, Y.V.; Shvetsov, G.G. Controlling the composition and quantity of oxide inclusions in a chromium steel. *Russ. Met.* **2007**, *2007*, 585–590. [[CrossRef](#)]
8. Das, N.K.; Sen, N.; Ghosh, M.; Sau, R. Effect of simultaneous addition of CaO-Al₂O₃ flux and CaSi on the modification of inclusions in aluminium-killed steel. *Scand. J. Met.* **2005**, *34*, 276–282. [[CrossRef](#)]
9. Li, X.; Jiang, Z.; Geng, X.; Chen, M.; Cui, S. Effect of Rare Earth-Magnesium Alloy on Inclusion Evolution in Industrial Production of Die Steel. *Steel Res. Int.* **2019**, *90*, 1900103. [[CrossRef](#)]
10. Zhang, Q.; Min, Y.; Xu, H.; Xu, J.; Liu, C. Formation and Evolution of Silicate Inclusions in Molten Steel by Magnesium Treatment. *ISIJ Int.* **2019**, *59*, 391–397. [[CrossRef](#)]
11. Pistorius, P.C. Steel-Slag Reactions in Ladle Metallurgy: Mass Transfer and Steel Cleanliness. In Proceedings of the International Congress on the Science & Technology of Steelmaking, Beijing, China, 12–14 May 2015.
12. Zhang, T.S.; Wang, D.Y.; Liu, C.W.; Jiang, M.F.; Ming, L.Ü.; Bo, W.A.; Zhang, S.X. Modification of Inclusions in Liquid Iron by Mg Treatment. *J. Iron Steel Res. Int.* **2014**, *21* (Suppl. S1), 99–103. [[CrossRef](#)]
13. Yang, S.F.; Li, J.S.; Wang, Z.F.; Li, J.; Lin, L. Modification of MgO·Al₂O₃ spinel inclusions in Al-killed steel by Ca-treatment. *Int. J. Miner. Metall. Mater.* **2011**, *18*, 18–23. [[CrossRef](#)]
14. Feng, J.; Bao, Y.; Cui, H. Effect of Magnesium on Modification of Inclusions in Low Carbon Aluminium-Killed Steel SPHC. *Teshugang* **2010**, *31*, 16–20.
15. Zheng, H.Y.; Guo, S.Q.; Qiao, M.R.; Qin, L.B.; Zou, X.J.; Ren, Z.M. Study on the Modification of Inclusions by Mg Treatment in GCr18Mo Bearing Steel. *Adv. Manuf.* **2019**, *7*, 438–447. [[CrossRef](#)]
16. Peng, Q.; Lei, Q.; Jian, Z. Effect of calcium treatment on inclusions in the steel LG510 and its thermodynamic analysis. *J. Wuhan Univ. Sci. Technol.* **2014**, *37*, 401–405.
17. Sun, W.; Wang, J.S.; Cao, L.J.; Xue, Q.G. Thermodynamic analysis on inclusion modification of magnesium treatment in bearing steel. *Liangang* **2010**, *26*, 41–43.
18. Tang, H.Y.; Li, J.S. Thermodynamic analysis on the formation mechanism of MgO·Al₂O₃ spinel type inclusions in casing steel. *Int. J. Miner. Metall. Mater.* **2010**, *17*, 34–40. [[CrossRef](#)]
19. Yang, J.; Yamasaki, T.; Kuwabara, M. Behavior of Inclusions in Deoxidation Process of Molten Steel with in Situ Produced Mg Vapor. *ISIJ Int.* **2007**, *47*, 699–708. [[CrossRef](#)]
20. Ma, W.; Bao, Y.; Wang, M.; Zhao, L. Effect of Mg and Ca Treatment on Behavior and Particle Size of Inclusions in Bearing Steels. *ISIJ Int.* **2014**, *54*, 536–542. [[CrossRef](#)]
21. Yu, Z.; Liu, C. Evolution Mechanism of Inclusions in Medium-Manganese Steel by Mg Treatment with Different Aluminum Contents. *Met. Mater. Trans. A* **2019**, *50*, 772–781. [[CrossRef](#)]
22. Takata, R.; Yang, J.; Kuwabara, M. Characteristics of Inclusions Generated during Al-Mg Complex Deoxidation of Molten Steel. *ISIJ Int.* **2007**, *47*, 1379–1386. [[CrossRef](#)]

23. Xi, Z.; Li, C.; Wang, L. A Kinetic Model for the Modification of Al_2O_3 Inclusions during Calcium Treatment in High-Carbon Hard Wire Steel. *Materials* **2021**, *14*, 1305. [[CrossRef](#)] [[PubMed](#)]
24. Itoh, H.; Hino, M.; Ban-Ya, S. Thermodynamics on the formation of spinel nonmetallic inclusion in liquid steel. *Metall. Mater. Trans. B* **1997**, *28*, 953–956. [[CrossRef](#)]
25. Gong, W.; Jiang, Z.; Zhang, L.; Chen, C.; Dong, Y. Influence of Mg addition on inclusions and mechanical properties of Cr12Mo1V1 steel under high pressure. *Mater. Sci. Eng. A* **2020**, *791*, 139410. [[CrossRef](#)]